Limiting glutamate transmission in a *Vglut2*-expressing subpopulation of the subthalamic nucleus is sufficient to cause hyperlocomotion

Nadine Schweizer[a,b,1], Stéfano Pupe[a,b,c,1], Emma Arvidsson[a,b], Karin Nordenankar[a,b], Casey J. A. Smith-Anttila[a,b], Souha Mahmoudi[d], Anna Andrén[a,b], Sylvie Dumas[e], Aparna Rajagopalan[a,b], Daniel Lévesque[d], Richardson N. Leão[b,c], and Åsa Wallén-Mackenzie[a,b,2]

Units of [a]Functional Neurobiology and [b]Developmental Genetics, Department of Neuroscience, Biomedical Center, Uppsala University, S-751 24 Uppsala, Sweden; [c]Brain Institute, Federal University of Rio Grande do Norte, 2155-59056-450 Natal-RN, Brazil; [d]Faculty of Pharmacy, Université de Montréal, Montréal, QC, Canada H3C 3J7; and [e]Oramacell, 75006 Paris, France

The subthalamic nucleus (STN) is a key area of the basal ganglia circuitry regulating movement. We identified a subpopulation of neurons within this structure that coexpresses *Vglut2* and *Pitx2*, and by conditional targeting of this subpopulation we reduced *Vglut2* expression levels in the STN by 40%, leaving *Pitx2* expression intact. This reduction diminished, yet did not eliminate, glutamatergic transmission in the substantia nigra pars reticulata and entopeduncular nucleus, two major targets of the STN. The knockout mice displayed hyperlocomotion and decreased latency in the initiation of movement while preserving normal gait and balance. Spatial cognition, social function, and level of impulsive choice also remained undisturbed. Furthermore, these mice showed reduced dopamine transporter binding and slower dopamine clearance in vivo, suggesting that *Vglut2*-expressing cells in the STN regulate dopaminergic transmission. Our results demonstrate that altering the contribution of a limited population within the STN is sufficient to achieve results similar to STN lesions and high-frequency stimulation, but with fewer side effects.

Parkinson disease | deep brain stimulation | vesicular transporter | optogenetics | striatum

The subthalamic nucleus (STN) has long been a structure of interest for researchers and clinicians alike. There is ample evidence that high-frequency stimulation of the STN improves symptoms such as tremor, rigidity, and slowness of movement, so called bradykinesia, in patients with Parkinson disease (see ref. 1 for review), but the mechanism through which this is achieved is still unknown. Some studies suggest that electrical stimulation causes a hyperexcitation of this structure (2), whereas others find evidence that the opposite is true (3–5). Other possible interpretations include the activation of the zona incerta, a neighboring white-matter structure (6) or of fibers coming from the motor cortex (7). Bilateral lesions of the STN improve locomotion (8), a result that is consistent with the inactivation hypothesis. However, previous studies have also found cognitive side effects when using high-frequency stimulation of the STN (9), findings supported by lesion studies in experimental animals, which led to abnormalities in operant tasks involving attention and impulsivity (10, 11). The projections of the STN to other regions help explain the multiple roles of this structure: It sends projections to other targets in the basal ganglia, such as the internal segment of the globus pallidus [also termed the entopeduncular nucleus (EP) in rodents] and the substantia nigra pars reticulata (SNr) (12, 13). The STN is also part of a circuit that includes the prefrontal cortex and the nucleus accumbens (14). It is currently unknown, however, whether these different roles reflect a heterogeneous population of cells, characterized by distinct gene expression. If that is the case, it would allow direct control over each cell population, facilitating the investigation of their respective roles. In rodents, the STN is believed to be composed

solely of glutamatergic neurons, characterized by expression of the subtype 2 *Vesicular glutamate transporter* (*Vglut2*), whereas the other two subtypes (*Vglut1* and *Vglut3*) have not been detected (15, 16). Selective targeted deletion of *Vglut2* expression in this nucleus would therefore provide a specific loss-of-function model that would bypass a common problem presented by traditional lesions with pharmacological agents, which have patterns of diffusion that likely affect surrounding structures (17). It is known, however, that *Vglut2* is expressed in many other parts of the brain (18), and a complete knockout in the mouse is not viable (19, 20). There is also evidence that the promoter driving expression of the *Paired-like homeodomain 2* (*Pitx2*) gene is strong in the mouse STN (21) but is also not specific to this structure and a full knockout of *Pitx2* expression results in premature death (22). To achieve the desired level of specificity, using a conditional knockout technique previously used to eliminate glutamatergic transmission in other cell types (23), we crossed *Pitx2-Cre* and *Vglut2-lox* mice, producing *Vglut2^f/f;Pitx2-Cre* conditional knockout (cKO) mice in which *Vglut2* expression in the STN was strongly reduced in comparison with expression levels in littermate control mice. To understand the physiological contribution of the selected subpopulation of STN cells, we characterized these cKO mice with regard to anatomical,

Significance

The subthalamic nucleus (STN) has an important role in locomotion, as evidenced by the successful use of high-frequency stimulation of this structure as treatment for Parkinson disease. There is considerable uncertainty, however, regarding the mechanism through which this effect is achieved. We identified a promoter diversity within this nucleus and observed a movement phenotype displayed as decreased latency in initiation of movement and increased locomotion in both horizontal and vertical planes as a consequence of blunting, but not eliminating, expression of *Vglut2* in the STN of mice. In contrast to various lesion and high-frequency-stimulation studies of the STN, our genetic approach leaves cognitive functions intact. Taken together, our findings could be important for advancing future therapeutic strategies.

NEUROSCIENCE

electrophysiological, and molecular properties, as well as their performance in a range of behavioral tasks.

Results

Pitx2-Cre–Mediated Targeting Shifts the Expression Profile of Vglut2 in the STN from High to Low Levels. The activity of the *Pitx2-Cre* transgene (21) was validated using the *Tau-mGFP* Cre-reporter transgene (24), which showed β-gal–immunopositive cell bodies in the STN (Fig. 1*A*) and GFP in the target areas of STN neurons, including the EP, corresponding to the internal segment of globus pallidus in primates (25) (Fig. 1*A*). β-gal was also detected in the mammillary nucleus (MN) and the posterior hypothalamus (PH), the two additional regions where *Pitx2* expression has been described (21). Mice gene-targeted for *Vglut2* specifically in *Pitx2-Cre*–expressing cells were produced by breeding *Pitx2-Cre* mice with *Vglut2*^f/f (19) mice, thereby producing cKO and control littermate mice. STN expression of all *Vglut* subtypes was analyzed on a single-cell level using multiplex single-cell RT-PCR analysis on freshly dissociated neurons from postnatal day (P) 1 and 20 control and cKO mice, detecting the *Vglut2* WT allele in 38% and 40% of control cells, respectively, and the KO allele in 15% of cKO cells at P1, which increased to 28% at P20. The

Fig. 1. The *Pitx2-Cre* transgene is expressed in the STN and mediates a shift in *Vglut2* mRNA levels and distribution. (*A*) Immunohistochemistry for β-gal (nuclear, *Left*) and GFP (projections, *Right*) on coronal mouse *Pitx2-Cre*^Tau-mGFP sections shows *Pitx2-Cre*–expressing cell nuclei in the STN (*Left*) and their projections to the EP (*Right*) target area. (*B*) Representative examples of in situ hybridization for *Vglut2* (magenta) and *Pitx2* (green) mRNA in STN (arrows) of Ctrl (*Upper row*) and cKO (*Lower row*), with a merge to the left. (*C*) Superposition of monochrome in situ images of STN (*Pitx2* mRNA, *Top row*; *Vglut2*, *Middle row*) with correlation values indicated according to correlation color scale to the right. mRNA level correlation analysis (*Pitx2* mRNA on *x* axis; *Vglut2* on *y* axis) from representative examples of Ctrl (*Left*) and cKO (*Right*). Pearson correlation coefficients for Ctrl and cKO r(Ctrl) = 0.8645 and r(cKO) = 0.71401, respectively. (*D*) Histograms of quantitative distribution of mRNA intensity; average expression level marked by yellow line, expression detection limit marked by gray dotted line. cKO, conditional knockout; Ctrl, control.

STN P20 cells were also analyzed for *Vglut1* expression, which was detected in both control and cKO cells, and for *Vglut3* expression, which was not detected at all (Fig. S1). In addition, analysis of MN and PH cells verified the expression of both *Vglut1* and *Vglut2* also in these areas and showed the incidence of the KO allele in 12% and 17% of *Vglut2*-expressing cells of cKO mice. In addition, all three areas contained cells coexpressing *Vglut1* and *Vglut2* (Fig. S1). Quantitative radioactive oligoprobe in situ hybridization was used to analyze the distribution of *Vglut2* mRNA in the STN, its overlap with *Pitx2*, and the extent of the *Vglut2* deletion in the adult mouse. Serial section analysis confirmed *Vglut2* expression in the adult STN and revealed a reduction of *Vglut2* expression in the STN of the cKO mice detected upon pure visual inspection (Fig. 1*B*). Closer examination of *Pitx2* and *Vglut2* expression in the STN by correlation analysis in each individual (two representative cases are shown in Fig. 1*C*) revealed a similar distribution of high and low expression values in control mice, whereas *Vglut2* expression was severely diminished in cKO mice, as reflected by the horizontally deflected correlation curve (Fig. 1*C*, *Right*). Subsequent quantitative evaluation of the difference in STN *Vglut2* mRNA expression between control and cKO brains showed a global ratio of STN vs. thalamus at 1.57 (± 0.16) in the control and 0.94 (± 0.12) in the cKO, a finding indicating a 40% decrease of *Vglut2* expression in the STN of the cKO brains. A similar quantification in the MN and PH did not show a significant decrease of *Vglut2* expression in either area (Fig. S1). A distribution analysis of *Pitx2* and *Vglut2* mRNA pattern in the STN revealed that both genes show a large dynamic range from low to high expression levels in the control, a range that remained the same for *Pitx2* in the cKO but that was altered for *Vglut2*, which instead showed a more homogenous *Vglut2* mRNA distribution with disappearance of high labelings (Fig. 1*D*). Further, the distribution of the labeling analyzed by quintiles showed that in the cKO the number of STN cells that expressed a very low level of mRNA was increased by 70%. The correlation analysis indicates that the *Pitx2* and *Vglut2* signals are highly mutually related in both control and cKO. The Pearson correlation ranged from 0.80 to 0.87 in control and 0.62 to 0.78 in cKO STN, the lower correlation level in the cKO being due to the change of the signal distribution for cKO and a usually higher variation, in relative terms, in weaker signal ranges. Moreover, the correlation data indicate that the decrease of *Vglut2* signal is not associated with a subregion of the STN but covers the extent of this structure.

Because multiple structures are innervated by the STN (13), to globally assess brain anatomy upon the limited deletion of *Vglut2* expression in the STN introduced here we analyzed serial sections spanning the entire brain upon in situ hybridization for excitatory (*Vglut1* and *Vglut2*), inhibitory (*glutamic acid decarboxylase*; *GAD*) and dopaminergic (*tyrosine hydroxylase*; *TH*) markers, respectively, all of which seemed normal (Fig. S2), apart from the selective reduction of *Vglut2* expression in the STN reported above.

Diminished, but Not Eliminated, Glutamatergic Transmission in the Main Target Areas of the STN. To understand the physiological consequences of the decreased *Vglut2* expression levels in the STN, we used parasagittal slices containing the STN, EP, and SNr (26) to assess synaptic currents in STN targets. Excitatory postsynaptic currents (EPSCs) in the EP and SNr were elicited by a single 400-μs shock delivered by a concentric electrode placed on the STN (Fig. 2*A*). EPSC amplitude in EP cells increased as stimulus intensity was increased in both control and cKO mice. However, the dependency of EPSC amplitude on stimulus intensity was greater in control mice (Fig. S3*A*). It has previously been shown that a single stimulation pulse generates STN-dependent multiple EPSCs (compound EPSCs) in postsynaptic neurons (26), and our data in control animals corroborate this finding (Fig. 2*A*). However, in cKO mice, EPSCs in both
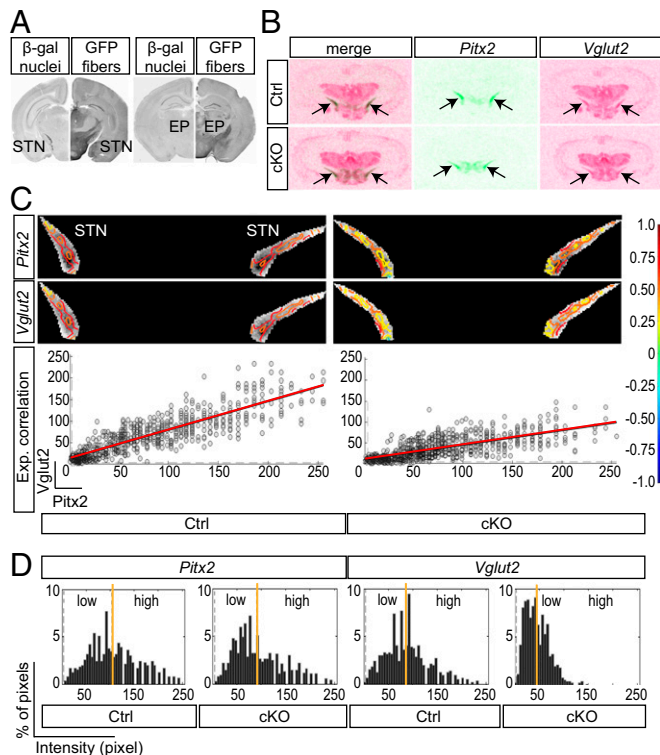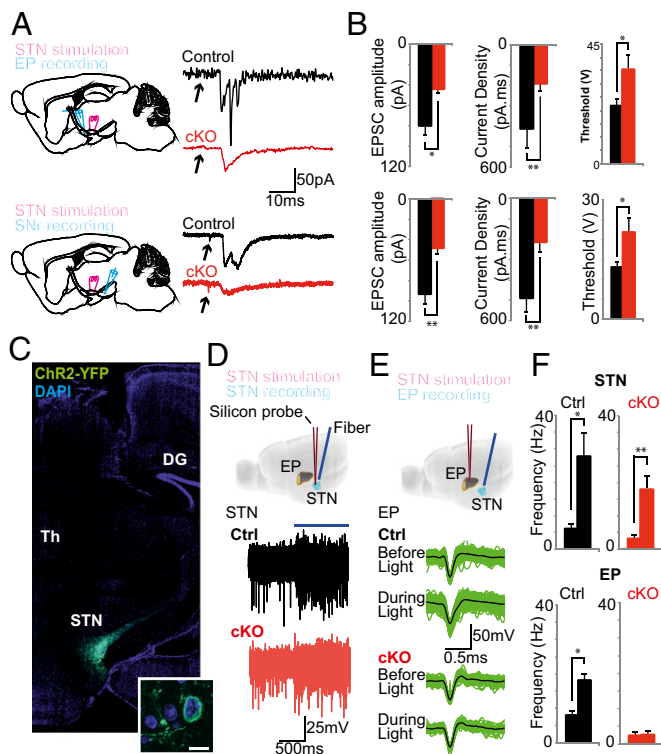
Fig. 2. Attenuation of *Vglut2* expression in the STN severely impairs synaptic communication postsynaptically. (*A*) (*Left*) Diagram showing stimulation and recording electrode placement in parasagittal slices containing the STN, EP, and SNr. (*Right*) Representative examples of synaptic currents elicited by STN stimulation (10% above threshold) in SNr and EP cells in control and cKO mice. (*B*) Mean EPSC amplitude, current density, and stimulation threshold for EP and SNr cells in control (black bars) and cKO (red bars) mice. (C) Photomicrograph showing representative *Pitx2-Cre*–driven ChR2 expression (through its reporting protein YFP) selectively in the STN with high magnification in inset. Dentate gyrus (DG) and thalamus (Th) are indicated for reference. (*D*) Example of extracellular recordings in the STN of control and cKO mice before and during light stimulation. (*E*) Single units isolated from EP recordings before and during light stimulation. (*F*) Summary of firing frequency in STN and EP recordings before and during light stimulation in control (black bars) and cKO (red bars) mice. *$P < 0.05$; **$P < 0.001$. cKO, conditional knockout; Ctrl, control.

EP and SNr consisted of a single event (Fig. 2*A*). Because compound EPSCs generate larger long-lasting currents (26), we compared EPSCs in control and cKO mice by measuring the area under the curve (current density) of EPSCs. Current densities in cKO were dramatically decreased in both EP and SNr cells (Fig. 2*B*, $P = 0.04$, $n = 20$ cells and $P = 0.004$, $n = 20$ cells, respectively). In addition, cKO mice displayed smaller amplitudes of the first EPSC peak in both nuclei (Fig. 2*B*, $P = 0.002$, $n = 20$ and $P = 0.001$, $n = 20$, respectively), whereas stimulation threshold (Fig. 2*B*, $P = 0.03$, $n = 20$ and $P = 0.02$, $n = 20$, respectively) and EPSC rise time (EP control/cKO 0.47 ± 0.07ms vs. 1.04 ± 0.13, $P = 0.001$, $n = 20$; SNr control/cKO 0.36 ± 0.10ms vs. 0.91 ± 0.11, $P = 0.002$, $n = 20$) were greater in EP and SNr cells of the cKO mice.

The impact of impaired synaptic transmission between the STN and postsynaptic targets in vivo was evaluated by light stimulation of STN cells transduced by stereotaxic injection of an adeno-associated virus vector (AAV) with Cre-dependent Channelrhodopsin 2 (ChR2). Injection of AAV-ChR2 in *Pitx2-Cre*–expressing control and cKO mice produced a robust expression of ChR2 and its reporter gene encoding the YFP in the STN (Fig. 2*C*). Using multisite probes with silicon substrate, we recorded single-unit activity in the STN and EP in response to light stimulation (Fig. 2 *D*

and *E*). Single 10-s-long light pulses caused a large increase in firing frequency of STN neurons in both control and cKO mice ($P = 0.01$, $n = 6$ units per two animals and $P = 0.003$, $n = 7$ units per two animals, respectively; Fig. 2*D*). However, light stimulation of STN in cKO mice caused no significant change in EP cell firing frequency ($n = 14$ cells per two animals; Fig. 2 *E* and *F*), whereas in control animals firing frequency was markedly increased ($P = 0.00003$, $n = 30$ cells per two animals; Fig. 2 *E* and *F*). These experiments verified that the targeted loss of *Vglut2* in the *Pitx2-Cre*–expressing cells of the STN severely affects the ability of STN to generate postsynaptic activity.

Normal Motor Coordination and Gait, but Accentuated Movement. Because the STN is heavily involved in motor behavior, we tested the *Vglut2$^{f/f,Pitx2-Cre}$* mouse line in a battery of motoric tests. Littermate control and cKO mice were tested on the balance beam, the rotarod, and in the treadmill to assess fine and crude motor coordination and gait, respectively. The time to cross the
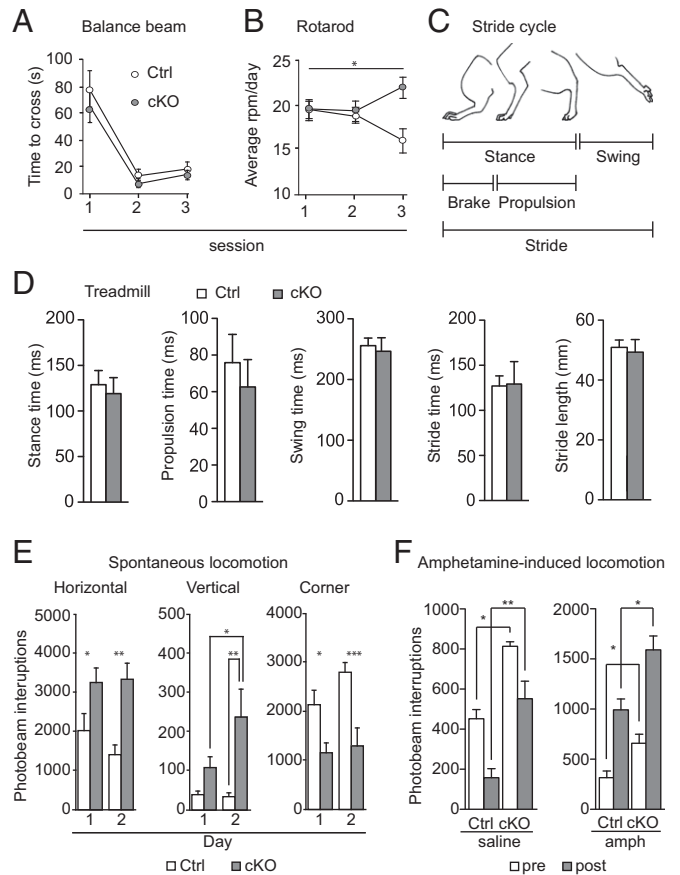

Fig. 3. Normal motor coordination and gait, and increased locomotion. (*A*) Fine motor coordination assessment on balance beam as measured by the time (seconds) needed to cross the beam. (*B*) Crude motor coordination assessment on rotarod, presented as mean of the rounds per minute (rpm) reached in three trials per day per animal on three consecutive days. (*C*) Illustration of the mouse stride cycle. (*D*) Stride cycle analysis on automated treadmill using averaged values for all four limbs for statistical analysis. Each mouse was trained to walk on the treadmill at speeds 10 and 15 cm/s and subsequently tested at 25 cm/s. (*E*) Horizontal (locomotion) and vertical (rearing) baseline activity, as well as resting (corner activity) during 60-min recordings in an open field setting, represented as number of photobeam interruptions. (*F*) Locomotion over 120-min recordings before (white bars) and after (gray bars) saline (*Left*) and amphetamine (*Right*) injections; 30 min preinjection, 90 min postinjection. *$P < 0.05$. cKO, conditional knockout; Ctrl, control.

NEUROSCIENCE

balance beam did not differ significantly between cKO and control mice, indicating that fine motor coordination is normal in cKO mice. Both groups improved over the three trial days ($P < 0.0001$; $F = 44.53$; df = 2) regardless of genotype ($P = 0.3046$; $F = 1.091$; df = 1) (Fig. 3A). During days 1 and 2, both cKO and control mice stayed on the rotarod up to similar speeds, whereas at day 3 cKO mice stayed on the rotarod at a significantly higher speed ($P = 0.0034$; $F = 6.104$; df = 2), indicating that the crude motor abilities of cKO mice are at least as good as those of controls (Fig. 3B). Gait analysis was performed in an automated treadmill measuring the different components of the entire stride cycle (illustrated in Fig. 3C). All stride cycle components were normal in the cKO mice [stance ($P = 0.1812$), additionally subdivided into brake and propulsion ($P = 0.2284$) and swing ($P = 0.8518$); stride as one unit ($P = 0.8518$ for stride time and $P = 0.7546$ for stride length)] (Fig. 3D). Movement was further addressed in paradigms of affective behavior. In the elevated plus maze, the time spent in each arm as well as the frequency of visits was similar between cKO and control mice, indicating a lack of anxiety-related behavior (Fig. S3B). However, we noted that the latency with which cKO mice moved out from the center and the latency to enter the outer open arm (OOA) of the maze was significantly shorter for the cKO mice ($P = 0.0115$ for center and $P = 0.0280$ for OOA). In the forced swim test, the time spent immobile during the second trial was significantly shorter for the cKO mice than for control littermates, showing an increase in overall swimming activity in the cKO group (Fig. S3C).

Next, we assessed various aspects of movement more directly in automated activity boxes. We observed that both horizontal and vertical movement was elevated in the cKO mice compared with control littermates. Locomotion was significantly increased in cKO mice compared with controls, both on days 1 and 2 in a 2-d trial ($P = 0.0034$ for days 1 and 2), whereas corner activity was significantly lower in cKO mice on both days ($P = 0.0008$; $q = 3.915$ and 5.668, respectively), showing that cKO mice spent more time in motion than their control littermates (Fig. 3E). Vertical movement (rearing) was also significantly elevated in the cKO mice on day 2 ($P = 0.0021$) and, moreover, significantly increased from day 1 to day 2 within the cKO group ($q = 3.799$) (Fig. 3E). Because it is well known that dopamine normally aids in the facilitation of movement, we used a pharmacological challenge approach composed of three different substances that alter extracellular dopamine levels by different mechanisms. First, we injected both control and cKO mice with saline and amphetamine (1.5 mg/kg, i.p.) and analyzed their locomotor response. Amphetamine strongly increases extracellular dopamine levels, and hence locomotion, by acting on both the cytoplasmic membrane dopamine transporter (DAT) and the vesicular counterpart (VMAT) (27). Both control and cKO mice showed the same level of response to amphetamine (Fig. 3F), leading to a *ca*. threefold increase in locomotion, but cKO mice displayed a higher level of activity already before injection ($P = 0.0286$ for saline, $P = 0.0286$ for amphetamine). This difference remained after both saline ($P = 0.0012$) and amphetamine ($P = 0.0106$) injection (Fig. 3F). A second batch of mice were then challenged with 7.5 and 15 mg/kg of GBR12783, a DAT-selective blocker; both doses led to a heightened response in cKO compared with control mice, but the difference failed to reach statistical significance (Fig. S4). After an injection of reserpine (2 mg/kg), a potent blocker of vesicular monoamine packaging by VMAT that causes catalepsy, a separate batch of mice showed no difference between controls and cKOs. Both groups showed a similar successive decrease in locomotion after reserpine injection (Fig. S4).

Normal Dopamine Receptor Distribution, but Reduced Striatal Dopamine Clearance in Vivo. To further explore the putative effect of the conditional STN targeting of *Vglut2* on dopamine neurotransmission in

the basal ganglia circuitry, we addressed various components of the dopamine system. In addition to the described expression analysis of *TH*, which encodes the rate-limiting enzyme for dopamine synthesis and showed normal distribution in the cKO brain (Fig. S2), a series of binding assays were performed and quantified in the SNc and four striatal target areas (illustrated in Fig. 4A). Ligand binding to D1R was normal in all four striatal areas examined as well as in the SNr, which was also quantified (Fig. S5). The same observation was made for the D2R, both in all striatal target areas analyzed as well as presynaptically in the dopamine cell bodies of the SNc (Fig. S5). In contrast, the binding capacity of DAT was significantly lower in the cKO in all striatal target areas examined but preserved in the cell bodies of the SNc, indicating a selective reduction of striatal
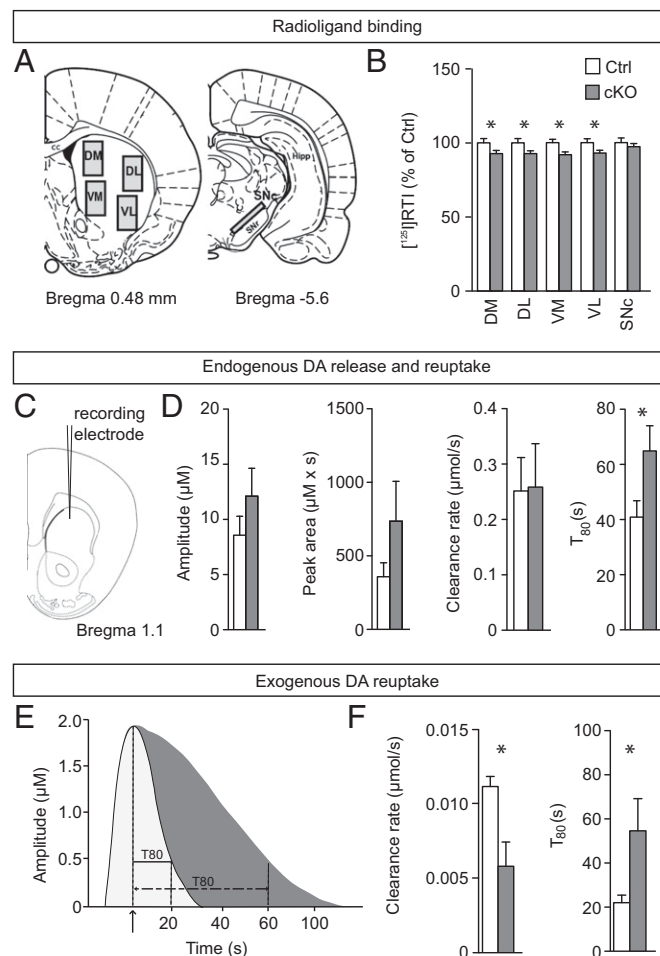

Fig. 4. Altered DAT levels and reduced dopamine clearance. (A) Illustration of areas selected for autoradiographic analysis: dorsomedial (DM), dorsolateral (DL), ventromedial (VM), and ventrolateral (VL) striatal area and the substantia nigra pars compacta (SNc). (B) Specific binding capacity levels expressed as percent of control for DAT-specific [^{125}I]RTI-121 ligand; for corresponding quantification of dopamine receptor 1 and 2 (D1R and D2) binding, see Fig. S5. (C) High-speed in vivo chronoamperometry recordings in the dorsal striatum of anesthetized mice. (D) KCl-evoked endogenous dopamine release and subsequent clearance: amplitude, peak area, clearance rate, and T_{80}. Note that T_{80} is significantly longer in cKO mice. (E) DAT-mediated clearance upon exogenous application of dopamine (maximum amplitude 2 μM) into the striatum; representative sample peaks of control (white) and cKO (gray). Note that dopamine clearance [represented by the time to reabsorb 80% of exogenous dopamine (T_{80})] is significantly prolonged in cKO mice. (F). Group averages for clearance rate (micromoles per second) (Left) and T_{80} (seconds) (Right). *$P < 0.05$; **$P < 0.01$. cKO, conditional knockout; Ctrl, control.

DAT expression in the cKO mice (Fig. 4B). To address whether dopamine kinetics is altered in the cKO mice, KCl-evoked dopamine release was measured and quantified in the dorsal striatum of anesthetized mice by high-speed in vivo chronoamperometry (Fig. 4C). No significant difference was found between control and cKO mice in dopamine amplitude, but a trend was observed in the cKO mice toward increased peak area and decreased clearance rate (Fig. 4D). A significant decrease was observed for dopamine clearance (T_{80}, $P = 0.0474$) (Fig. 4D). Local striatal application of exogenous dopamine also revealed significantly reduced clearance in the cKO mice (Fig. 4E; representative peaks derived from control and cKO mice). Significantly lower clearance rate ($P = 0.0317$) (Fig. 4F) as well as prolonged time to clear 80% of dopamine from the extracellular space (T_{80}, $P = 0.0451$) (Fig. 4F) were observed. Targeting Vglut2 in the STN thus leads to an effect on DAT activity that is likely to contribute to the hyperlocomotion phenotype observed.

Preserved Spatial Memory, Level of Impulsivity, Cognitive Flexibility, and Social Dominance. To analyze cognitive behavior in the cKO mice, spatial working and reference memory was measured in the radial eight-arm maze. cKO mice did not make more working memory or reference memory errors than controls; however, they had a significantly increased number of trials that were not completed (Fig. S6). We also used the delay discounting task, a paradigm that allows the animal to freely choose between a small but immediate reward and a larger, but delayed, one. The cKO mice did not differ significantly from controls in their ability to wait for a larger reward, but they refrained from choosing in response to the light stimulus more often. All animals registered similar omissions to collect the earned reward, average latencies to choose or collect rewards, and inappropriate head entries at the small reward side and inactive holes (Fig. S7).

Discussion

Contrary to what was previously reported (15, 16), we found that the STN has not one, but at least three main populations of glutamatergic cells, as characterized by their expression of either Vglut1 or Vglut2 or coexpression of both. Vglut2 is expressed at higher, and thus more readily detectable, levels than Vglut1 and is strongly correlated with Pitx2 expression. Despite the restricted reduction of Vglut2 expression in the STN of our cKO mice, leaving about two-thirds of the original Vglut2 expression levels, it gave rise to severely disrupted communication with the main target areas, the EP and the SNr, and the mice displayed a strong movement-specific phenotype while preserving, with minor exceptions, normal cognitive and affective behavior. In addition to the reduced glutamatergic tone in the SNr and EP, decreased DAT levels and slower dopamine reuptake support an indication of increased extracellular dopamine in the striatum, likely related to the observed hyperlocomotion. Altogether, our results demonstrate that shifting the Vglut2 expression profile in the STN from high- to low-level expression is sufficient to cause behavioral consequences comparable with much larger and indiscriminate lesions in this area.

Since the discovery of the beneficial clinical effects of STN high-frequency stimulation, this nucleus has been the subject of hundreds of studies attempting to explain the phenomenon (28). Valuable efforts have been made in characterizing the anatomical (29) and electrophysiological (30) properties of neurons within this structure. Recently, Favier et al. (31) identified altered protein levels of VGLUT1 and VGLUT2 in multiple brain areas upon STN high-frequency stimulation. The identification of promoter-specific subgroups of neurons within the STN itself, however, has been somewhat neglected, likely owing to the homogeneity of the STN (having only one type of neurotransmitter, glutamate), and the relatively recent discovery of different glutamatergic transporters. Compared with previous attempts that performed a broad Vglut characterization of several brain areas at once (15, 16, 32),

we focused our efforts specifically on the STN and quantified the expression of Vglut1 and Vglut2 through both in situ hybridization and single-cell RT-PCR techniques. Whereas Vglut2 expression was easily detected by both techniques, Vglut1 expression—not detected by in situ hybridization analysis—could be quantified by multiplex single-cell RT-PCR. We found a partial overlap between the expression of both transporters, a pattern that is also found in other areas of the central nervous system (33, 34). The advantage of characterizing the expression pattern of promoters is the ability to subsequently manipulate them, an approach we took here by blunting glutamatergic release in Vglut2-expressing cells that were also positive for Pitx2. This is the first description, to our knowledge, of a behavioral role for a subpopulation of neurons within the STN. Our results are comparable to those obtained by traditional methods of lesioning this nucleus, in which animals display a consistent improvement in locomotion (35), and also clearly observed in experiments with high-frequency stimulation of the STN (36, 37). Although we cannot determine whether disabling Vglut2-expressing neurons is necessary for this behavioral effect, we now have evidence that it is a sufficient condition. Moreover, the effect we observe here does seem specific to the role of Vglut2 itself in the STN, and not to a general decrease in glutamatergic signaling: Vglut2-heterozygous mice, in which all glutamatergic transmission mediated by this transporter is reduced by up to 50%, present no abnormalities in locomotion (20), and the same is true for mice heterozygous for Vglut1 (38). Therefore, it is likely that the effects we achieved are due to a characteristic property of the cKO cells, such as their local connectivity or projection targets. The experiments we performed regarding synaptic activity in the two major targets of the STN corroborate this interpretation. The cKO mice showed a strong reduction in the excitatory activity the STN could produce on the EP and the SNr, as evidenced by both in vitro and in vivo electrophysiology. The latter experiments, using ChR2 expression selectively in Pitx2-Cre–expressing cells of the STN, could confirm that these neurons are normally able to induce increased activity in the STN targets, but that this function was lost after Vglut2 conditional deletion.

Considering the classic model describing a direct and an indirect pathway through the basal ganglia, we suggest that the locomotor effects we observed were likely mediated by this disruption in the indirect pathway, weakening the STN chronic excitation on the SNr and EP and, thus, decreasing the total inhibitory output these structures have on the thalamus. Additionally, consistent with high-frequency stimulation studies (39), no difference was found in the levels of dopamine receptor binding in the dorsal striatum; the altered DAT levels, however, in combination with slower dopamine clearance, are suggestive of overall elevated extracellular striatal dopamine levels. Besides locomotor activity, the behavioral tasks we performed generally did not show any differences between cKOs and controls, showing that the role of Vglut2-expressing cells in the STN seems to be closely related to locomotion. One notable exception was the forced swim test, in which the knockout mice spent more time active, a finding that suggests that, unlike interventions such as high-frequency stimulation of the STN (39), our cKOs do not show increased depression-like behavioral symptoms, but rather the opposite. In humans, lesions of the STN have also been reported to improve depression symptoms (8). The effect we saw could be due to some particular pattern of projections of the Vglut2 population of cells compared with other neurons in the STN, or simply due to the fact that the cKO mice are more active in general, possibly even during the water-based test. Aside from this, it seems our intervention was largely limited to locomotor consequences, presenting none of the affective or cognitive impairments observed in other experiments. It is possible to speculate that this promoter-based approach to decreasing STN function could be a way of avoiding some of the side effects commonly seen in treatments that require lesions or high-frequency stimulation of this nucleus.

NEUROSCIENCE

Perhaps the most severe limitation in our study is the use of knockout animals, a method that does not discriminate between developmental and acute effects. However, it can be argued that, given the progressive nature of our knockout, this limitation was not as worrisome as most knockout techniques. Another limitation is the fact that we also targeted some neurons in other parts of the brain, in particular the PH and the MN, even though neither area showed significantly reduced *Vglut2* expression levels as detected by quantitative in situ hybridization. These structures are not traditionally associated with locomotion, and lesion studies also do not support a contributing role as to the phenotype of our cKO mice (39, 40), but every manipulation can have unforeseeable consequences, and we cannot rule out that they are also involved in some of the results we reported. It is conceivable that our results could translate to other animals, and to humans as well. In monkeys, the STN seems to be composed almost exclusively of *Vglut2*-expressing neurons (40), although this report relies solely on in situ hybridization, which we showed to be unreliable to detect *Vglut1* in mice. Silencing a particular subset of cells through genetic or pharmacological means could be feasible in the future and might be clinically relevant for Parkinson disease.

Materials and Methods

All mice used in the study were housed in accordance with the Swedish regulation guidelines (Animal Welfare Act SFS 1998:56) and European Union legislation (Convention ETS123 and Directive 2010/63/EU). The *Vglut2^{f/f;Pitx2}* mouse line was produced by breeding the Pitx2-Cre mice (21) to *Vglut2^{f/f}* (19) mice, thereby generating cKO (*Vglut2^{f/f;Pitx2-Cre+}*) and controls (*Vglut2^{f/f;Pitx2-Cre-}* and *Vglut2^{wt/wt;Pitx2-Cre+}*) as littermates with the identical genetic background. For a detailed outline of the experimental setups, see *SI Materials and Methods*.

1. Benabid AL, Chabardes S, Mitrofanis J, Pollak P (2009) Deep brain stimulation of the subthalamic nucleus for the treatment of Parkinson's disease. *Lancet Neurol* 8(1):67–81.
2. Windels F, et al. (2000) Effects of high frequency stimulation of subthalamic nucleus on extracellular glutamate and GABA in substantia nigra and globus pallidus in the normal rat. *Eur J Neurosci* 12(11):4141–4146.
3. Benazzouz A, et al. (2000) Effect of high-frequency stimulation of the subthalamic nucleus on the neuronal activities of the substantia nigra pars reticulata and ventrolateral nucleus of the thalamus in the rat. *Neuroscience* 99(2):289–295.
4. Magariños-Ascone C, Pazo JH, Macadar O, Buño W (2002) High-frequency stimulation of the subthalamic nucleus silences subthalamic neurons: A possible cellular mechanism in Parkinson's disease. *Neuroscience* 115(4):1109–1117.
5. Tai C-H, et al. (2003) Electrophysiological and metabolic evidence that high-frequency stimulation of the subthalamic nucleus bridles neuronal activity in the subthalamic nucleus and the substantia nigra reticulata. *FASEB J* 17(13):1820–1830.
6. Plaha P, Ben-Shlomo Y, Patel NK, Gill SS (2006) Stimulation of the caudal zona incerta is superior to stimulation of the subthalamic nucleus in improving contralateral parkinsonism. *Brain* 129(Pt 7):1732–1747.
7. Gradinaru V, Mogri M, Thompson KR, Henderson JM, Deisseroth K (2009) Optical deconstruction of parkinsonian neural circuitry. *Science* 324(5925):354–359.
8. Alvarez L, et al. (2005) Bilateral subthalamotomy in Parkinson's disease: Initial and long-term response. *Brain* 128(Pt 3):570–583.
9. Parsons TD, Rogers SA, Braaten AJ, Woods SP, Tröster AI (2006) Cognitive sequelae of subthalamic nucleus deep brain stimulation in Parkinson's disease: A meta-analysis. *Lancet Neurol* 5(7):578–588.
10. Winstanley CA, Baunez C, Theobald DEH, Robbins TW (2005) Lesions to the subthalamic nucleus decrease impulsive choice but impair autoshaping in rats: The importance of the basal ganglia in Pavlovian conditioning and impulse control. *Eur J Neurosci* 21(11):3107–3116.
11. Baunez C, Robbins TW (1997) Bilateral lesions of the subthalamic nucleus induce multiple deficits in an attentional task in rats. *Eur J Neurosci* 9(10):2086–2099.
12. Van Der Kooy D, Hattori T (1980) Single subthalamic nucleus neurons project to both the globus pallidus and substantia nigra in rat. *J Comp Neurol* 192(4):751–768.
13. Kita H, Kitai ST (1987) Efferent projections of the subthalamic nucleus in the rat: light and electron microscopic analysis with the PHA-L method. *J Comp Neurol* 260(3):435–452.
14. Maurice N, Deniau JM, Menetrey A, Glowinski J, Thierry AM (1998) Prefrontal cortex-basal ganglia circuits in the rat: Involvement of ventral pallidum and subthalamic nucleus. *Synapse* 29(4):363–370.
15. Hisano S (2003) Vesicular glutamate transporters in the brain. *Anat Sci Int* 78(4):191–204.
16. Barroso-Chinea P, et al. (2007) Expression of the mRNAs encoding for the vesicular glutamate transporters 1 and 2 in the rat thalamus. *J Comp Neurol* 501(5):703–715.
17. Köhler C, Schwarcz R (1983) Comparison of ibotenate and kainate neurotoxicity in rat brain: A histological study. *Neuroscience* 8(4):819–835.
18. Lein ES, et al. (2007) Genome-wide atlas of gene expression in the adult mouse brain. *Nature* 445(7124):168–176.
19. Wallén-Mackenzie Å, et al. (2006) Vesicular glutamate transporter 2 is required for central respiratory rhythm generation but not for locomotor central pattern generation. *J Neurosci* 26(47):12294–12307.
20. Moechars D, et al. (2006) Vesicular glutamate transporter VGLUT2 expression levels control quantal size and neuropathic pain. *J Neurosci* 26(46):12055–12066.
21. Martin DM, et al. (2004) PITX2 is required for normal development of neurons in the mouse subthalamic nucleus and midbrain. *Dev Biol* 267(1):93–108.
22. Sclafani AM, et al. (2006) Nestin-Cre mediated deletion of Pitx2 in the mouse. *Genesis* 44(7):336–344.
23. Birgner C, et al. (2010) VGLUT2 in dopamine neurons is required for psychostimulant-induced behavioral activation. *Proc Natl Acad Sci USA* 107(1):389–394.
24. Hippenmeyer S, et al. (2005) A developmental switch in the response of DRG neurons to ETS transcription factor signaling. *PLoS Biol* 3(5):e159.
25. Gerfen CR (1992) The neostriatal mosaic: Multiple levels of compartmental organization. *Trends Neurosci* 15(4):133–139.
26. Ammari R, Lopez C, Bioulac B, Garcia L, Hammond C (2010) Subthalamic nucleus evokes similar long lasting glutamatergic excitations in pallidal, entopeduncular and nigral neurons in the basal ganglia slice. *Neuroscience* 166(3):808–818.
27. Sulzer D, Sonders MS, Poulsen NW, Galli A (2005) Mechanisms of neurotransmitter release by amphetamines: A review. *Prog Neurobiol* 75(6):406–433.
28. McIntyre CC, Savasta M, Kerkerian-Le Goff L, Vitek JL (2004) Uncovering the mechanism(s) of action of deep brain stimulation: Activation, inhibition, or both. *Clin Neurophysiol* 115(6):1239–1248.
29. Nauta HJW, Cole M (1978) Efferent projections of the subthalamic nucleus: An autoradiographic study in monkey and cat. *J Comp Neurol* 180(1):1–16.
30. Beurrier C, Congar P, Bioulac B, Hammond C (1999) Subthalamic nucleus neurons switch from single-spike activity to burst-firing mode. *J Neurosci* 19(2):599–609.
31. Favier M, et al. (2013) High-frequency stimulation of the subthalamic nucleus modifies the expression of vesicular glutamate transporters in basal ganglia in a rat model of Parkinson's disease. *BMC Neurosci* 14(1):152.
32. Hur EE, Zaborszky L (2005) Vglut2 afferents to the medial prefrontal and primary somatosensory cortices: A combined retrograde tracing in situ hybridization study [corrected]. *J Comp Neurol* 483(3):351–373.
33. Kaneko T, Fujiyama F, Hioki H (2002) Immunohistochemical localization of candidates for vesicular glutamate transporters in the rat brain. *J Comp Neurol* 444(1):39–62.
34. Todd AJ, et al. (2003) The expression of vesicular glutamate transporters VGLUT1 and VGLUT2 in neurochemically defined axonal populations in the rat spinal cord with emphasis on the dorsal horn. *Eur J Neurosci* 17(1):13–27.
35. Bergman H, Wichmann T, DeLong MR (1990) Reversal of experimental parkinsonism by lesions of the subthalamic nucleus. *Science* 249(4975):1436–1438.
36. Shi L-H, et al. (2004) High-frequency stimulation of the subthalamic nucleus reverses limb-use asymmetry in rats with unilateral 6-hydroxydopamine lesions. *Brain Res* 1013(1):98–106.
37. Vlamings R, et al. (2007) High frequency stimulation of the subthalamic nucleus improves speed of locomotion but impairs forelimb movement in Parkinsonian rats. *Neuroscience* 148(3):815–823.
38. Tordera RM, et al. (2007) Enhanced anxiety, depressive-like behaviour and impaired recognition memory in mice with reduced expression of the vesicular glutamate transporter 1 (VGLUT1). *Eur J Neurosci* 25(1):281–290.
39. Temel Y, et al. (2007) Inhibition of 5-HT neuron activity and induction of depressive-like behavior by high-frequency stimulation of the subthalamic nucleus. *Proc Natl Acad Sci USA* 104(43):17087–17092.
40. Rico AJ, et al. (2010) A direct projection from the subthalamic nucleus to the ventral thalamus in monkeys. *Neurobiol Dis* 39(3):381–392.